Journal of Zhejiang University-SCIENCE A (Applied Physics & Engineering)
ISSN 1673-565X (Print); ISSN 1862-1775 (Online)
www.zju.edu.cn/jzus; www.springerlink.com
E-mail: jzus@zju.edu.cn

Effect of template shape on metal nanoimprinting: a dislocation dynamics study*

Yun-he ZHANG, Lucia NICOLA†‡

(*Department of Materials Science and Engineering, Delft University of Technology, 2628 CD Delft, the Netherlands*)

†E-mail: l.nicola@tudelft.nl

Received Apr. 16, 2010; Revision accepted July 15, 2010; Crosschecked Sept. 19, 2010

Abstract: Dislocation dynamics simulations are performed to investigate the effect of template shape on the nanoimprinting of metal layers. To this end, metal thin films are imprinted by a rigid template made of an array of equispaced indenters of various shapes, i.e., rectangular, wedge, and circular. The geometry of the indenters is chosen such that the contact area is approximately the same at the final imprinting depth. Results show that, for all template shapes, the final patterns strongly depend on the dislocation activity, and that each imprint differs from the neighboring ones. Large material pile ups appear between the imprints, such that polishing of the metal layer is suggested for application of the patterns in electronics. Rectangular indenters require the lowest imprinting force and achieve the deepest retained imprints.

Key words: Nanoimprinting, Dislocation dynamics, Simulations
doi:10.1631/jzus.A1000175 **Document code:** A **CLC number:** TB3

1 Introduction

Metal nanoimprinting is a fabrication technique currently applied to a wide variety of miniaturized systems (Guo, 2007). The pattern is generally transferred from a rigid template onto a polymer or photoresist, and afterwards etched into the metal. A different approach is to transfer the pattern directly from the template onto a metal layer by plastically deforming the metal (Cross *et al*., 2006). The objective of this study is to investigate numerically the capability of the metal to retain imprints when directly indented by a template with protruding contacts of various shapes. Specifically, each protruding contact is either rectangular, circular, or wedge shaped.

The challenge originates from the size-dependent plastic properties of metal layers at the sub-micron size scale (Zong *et al*., 2006), for which conventional classical plasticity models have proven to be non-suitable. The approach used in this study is discrete dislocation plasticity (van der Giessen and Needleman, 1995), where plasticity in the metal film originates from the collective motion of discrete dislocations. This simulation technique has been successfully employed in the prediction of size effects in metals by indentation (Widjaja *et al*., 2005) as well as by imprinting with equispaced contacts (Nicola *et al*., 2008; Zhang *et al*., 2010).

2 Methods

An infinitely long thin film of height h_f=200 nm on an elastic substrate of height h_s=50 nm is imprinted by a rigid template (Fig. 1). If the choice of a thicker elastic substrate was made, shallower retained imprints would be obtained for the same imprinting depth. The template is made of arrays of equispaced indenters of different shapes, i.e., rectangular, wedge, and circular. Imprinting occurs at a constant velocity $\dot{u}$ =5×10^6 nm/s to the final imprinting depth u_{max}=

‡ Corresponding author
* Project (No. VENI 08120) supported by the Dutch National Scientific Foundation NWO and Dutch Technology Foundation STW

10 nm. The 2D analysis is performed on a unit cell of width W comprising n indenters with center-to-center spacing w. Contact between template and metal is assumed to be perfectly sticking during indentation by prescribing

$$\dot{u}_1(x_1,h)=0,\quad \dot{u}_2(x_1,h)=-\dot{u},\quad x_1\in A_{\text{contact}},\qquad (1)$$

where $h=h_s+h_f$, and A_{contact} is the surface in contact. The remaining top surface is free:

$$\sigma_{12}(x_1,h)=\sigma_{22}(x_1,h)=0,\quad x_1\notin A_{\text{contact}}.$$

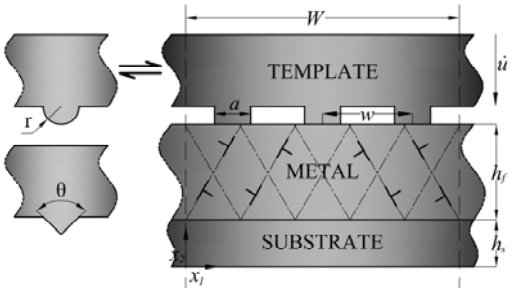

Fig. 1 2D model of a metal thin film on substrate imprinted by a rigid template with protruding contacts with rectangular, wedge, or circular shapes

Because of the sticking nature of the contact, the bottom surface cannot expand during imprinting. Periodic boundary conditions are imposed at the left and right boundaries of the unit cell:

$$\begin{cases}\dot{u}_1(0,x_2)-\dot{u}_1(W,x_2)=0,\\ \dot{u}_2(0,x_2)-\dot{u}_2(W,x_2)=0,\ \forall x_2.\end{cases}\qquad (2)$$

The metal layer is taken to have the elastic properties of aluminum: Young's modulus E=70 GPa and Possion's ratio υ=0.33. For simplicity, plasticity in the substrate is ignored and the substrate is assigned the same elastic constants as the film. Equispaced dislocation sources with critical strength τ_{nuc}= 50 MPa are positioned at the top surface. The source density is ρ_{nuc}=0.14/nm. Dislocations can glide on two sets of parallel slip planes, each of which contains one dislocation source. The slip planes are oriented alternatively either at 54.75° or at 125.25° with the x_1-axis. This mimics in two dimensions the slip planes for easy glide of a face centered cubic (FCC) crystal imprinted along the [010] direction (Rice, 1987). The magnitude of the Burgers vector is b=0.25 nm. Obstacles with strength τ_{obs}=150 MPa are randomly distributed in the metal with density ρ_{obs}=30/μm^2. Dislocation nucleation occurs when the resolved shear stress on a source exceeds its critical strength during the nucleation time $t_{\text{nuc}}=1\times10^{-8}$ s. Then two dislocations with opposite Burgers vector are generated at a distance L_{nuc}. The glide velocity v^I of the Ith dislocation is proportional to the Peach-Koehler force f^I according to

$$f^I=Bv^I\qquad (3)$$

with the drag coefficient $B=10^{-4}$ Pa·s.

3 Results and discussion

Simulations are performed for templates of different shapes, all having indenters spaced by w= 400 nm. Each unit cell contains six indenters to reduce statistical variations.

The geometric characteristics of the indenters are the followings: the width of the rectangular indenter is a=50 nm, the angle of the wedge indenter is θ=160°, and the radius of the circular indenter is r=130 nm. The particular geometries are chosen to give approximately the same true contact area (projected on the x_1-axis) for the three indenter shapes at the maximum imprinting depth. Force-displacement curves during indentation and unloading are shown in Fig. 2a. The imprinting force is calculated at the top surface as

$$F:=-\int_{A_{\text{contact}}}\sigma_{22}(x_1,h)\mathrm{d}x_1.$$

To reach the maximum imprinting depth, a force of approximately 1380 N/m is required for wedge and circular indenters, while a lower force, 840 N/m, is needed for the rectangular indenter. This is a rather unexpected result in that the contact area for the rectangular indenter is larger than that of the other indenters for u<10 nm. This can be seen in Fig. 2b, which gives the evolution of the contact area during loading and unloading. The contact area for the rectangular indenter during imprinting is clearly constant and equal to a=50 nm. In the case of the wedge and circular indenters, the contact area plotted here is the real area of contact between the indenter and the

metal layer, projected in x_1-direction. The contact area increases at a larger rate when the indenter is circular.

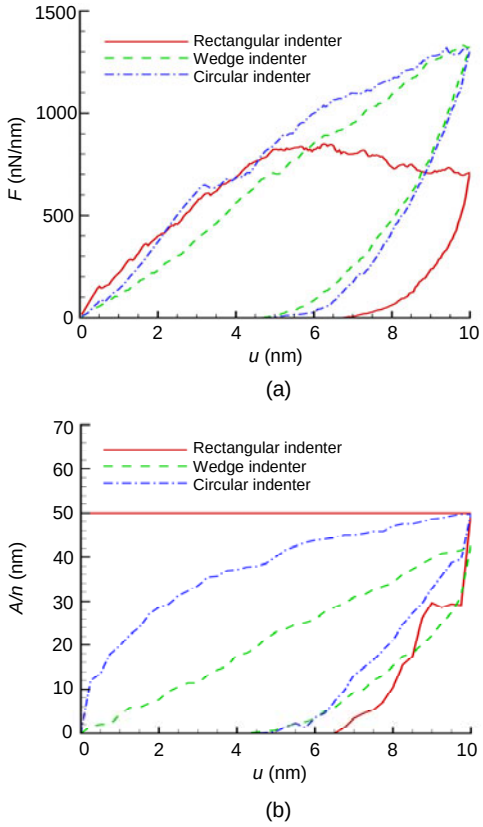

Fig. 2 The imprinting force (a) and the true contact area (b) projected on the x_1-axis for different indenters shapes

Fig. 3a shows the metal top surface profile at the maximum imprinting depth u_{max}=10 nm. The material in between imprints forms, in all cases, very pronounced pile-ups with irregular shape. The irregular shape of the pile ups and imprints is caused by the discrete nature of sources and dislocations. The dislocation sources distribution is non-symmetric and therefore causes asymmetry in the deformation of the metal film. Also, a large number of dislocations glide out of the metal free surface during indentation and leave displacement steps there. These dislocation steps are also responsible for the discontinuous evolution of the contact area for the cases of wedge and circular indenters.

Note that the profiles in Fig. 3a are shown using independent axes for a better visibility of the imprints. In fact, the correct proportions of each imprint is shown in Fig. 3b; i.e., the real imprint is wider than it is deep (the imprinting depth is only u=10 nm, while the projected contact area is approximately 50 nm). After unloading and relaxation, part of the deformation is lost due to elastic spring-back. The retained imprints are shown in Fig. 4. During unloading and relaxation, the metal profile becomes even rougher and more irregular. This is particularly true for the imprints obtained by rectangular indenters, which are

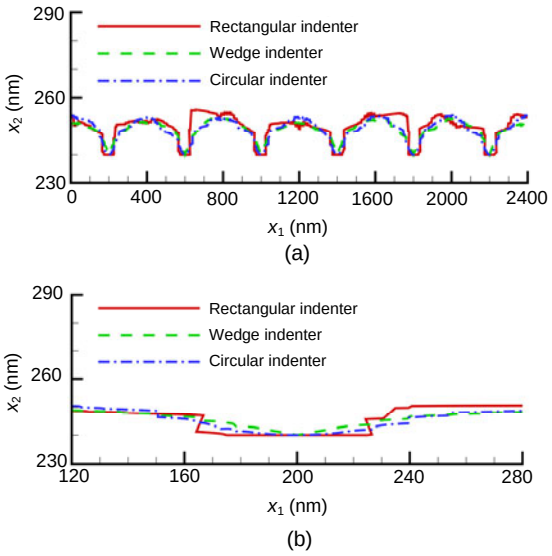

Fig. 3 The top surface profile for different shapes at the maximum imprinting depth u_{max}=10 nm (a); One of the imprints in the unit cell (dependent axes) (b)

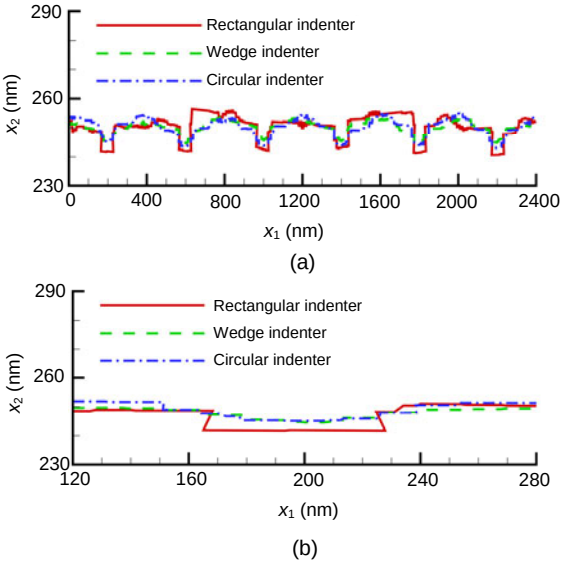

Fig. 4 The top surface profile for different shapes after unloading and relaxation (a); One of the imprints (dependent axes) (b)

also the deepest. Since most electronic applications require bonding of the patterned metal film with other layers, polishing of the final surface is advised to flatten the top surface.

To demonstrate how the material piles up in between imprints during indentation, Fig. 5 shows the displacement distribution in the x_2-direction and the corresponding dislocation distribution at the maximum imprinting depth. The flow of material appears the most evident in the case of the rectangular indenters (Fig. 5a), where well-defined triangular regions of materials are pushed up by the imprinting. The reason the triangular regions are so clearly defined is that the contact area is constant for the rectangular indenters during imprinting; therefore, the locations of high stress concentration do not move. As a consequence, only a few dislocation sources, those that are in the highly stressed region close to the edges of the contact, are very active and slip occurs on preferential slip planes. These are the slip planes located at the borders of the triangular regions. The dislocation density in the metal is rather low, since many dislocations have left the material through the free top surface or have been absorbed into the interface between the film and substrate.

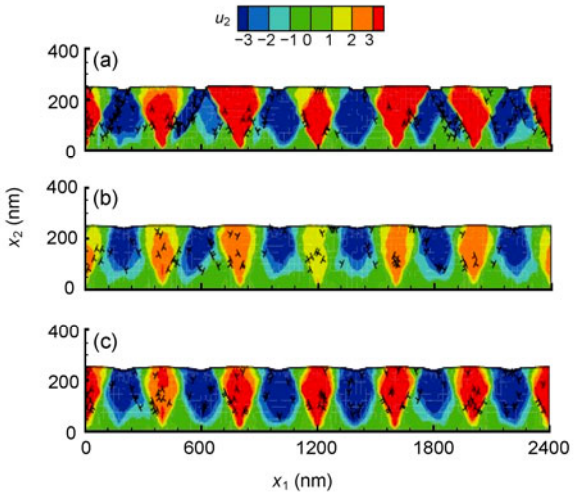

Fig. 5 The distribution of displacement in x_2-direction for rectangular (a), wedge (b), and circular indenters (c) at the maximum imprinting depth

To better characterize the final patterns, Table 1 gives the depth of the center of the imprint d_{imp}, measured from the original film height h=250 nm, and averaged over the imprints in the unit cell; i.e.,

$$d_{\text{imp}} = \frac{1}{n}\sum_{I=1}^{n}\left|h - x_2\left(wI - \frac{w}{2}\right)\right|,$$

where n is the number of indenters in the unit cell. The deepest imprints are obtained by the rectangular indenters, while the shallowest by the circular indenter. We measure the width of the imprint w_{imp} at h=250 nm, and average over the number of imprints in the unit cell. The results in Table 1 show that the opening of the imprints has, for all templates, a rather large standard deviation. In the case of the rectangular indenters, it is noteworthy that on average the opening of the imprint is twice the size of the indenter.

Table 1 Average imprint depth and width

Shape	d_{imp} (nm)	w_{imp} (nm)
Rectangular	8.08±9.96%	107.28±65.28%
Wedge	5.02±9.39%	153.27±38.34%
Circular	6.19±12.10%	156.92±41.28%

4 Conclusions

We have presented discrete dislocation simulations of the nanoimprinting of metallic thin films by a rigid template. The template is made of an array of equispaced indenters of various shapes, namely rectangular, wedge, and circular. The shape of the indenters is chosen such that the final contact area is approximately the same. Results show that for the chosen indenters spacing, w=400 nm, the template with rectangular indenters appear the most suitable to pattern the metal, because: (1) it requires a lower imprinting force than the other templates; (2) it produces the deepest retained imprints.

The reason is that imprinting with rectangular indenters occurs at a constant contact area. Therefore, slip occurs only on selected slip planes, facilitating push up of material between the imprints.

Also, for all template shapes considered:

1. The final surface profiles are strongly affected by the dislocation activity.

2. The obtained patterns are rather irregular: each imprint is different from the neighboring ones.

3. Material pile ups between indenters are very pronounced. For electronic applications the metal would require polishing of the top surface.

References

Cross, G.L.W., O'Connell, B.S., Özer, H.O., Pethica, J.B., 2007. Room temperature mechanical thinning and imprinting of solid films. *Nano Letters*, **7**(2):357-362.

Guo, L.J., 2007. Nanoimprint lithography: methods and material requirements. *Advanced Materials*, **19**(4):495-513. [doi:10.1002/adma.200600882]

Nicola, L., Bower, A.F., Kim, K.S., Needleman, A., van der Giessen, E., 2008. Multi-asperity contact: A comparison between discrete dislocation and crystal plasticity predictions. *Philosophical Magazine*, **88**(30-32):3713-3729. [doi:10.1080/14786430802566372]

Rice, J.R., 1987. Tensile crack tip fields in elastic-ideally plastic crystals. *Mechanics of Materials*, **6**(4):317-335. [doi:10.1016/0167-6636(87)90030-5]

van der Giessen, E., Needleman, A., 1995. Discrete dislocation plasticity: a simple planar model. *Modelling and Simulation in Materials Science and Engineering*, **3**(5):689-735. [doi:10.1088/0965-0393/3/5/008]

Widjaja, A., van der Giessen, E., Needleman, A., 2005. Discrete dislocation modelling of submicron indentation. *Materials Science and Engineering: A*, **400-401**(25):456-459. [doi:10.1016/j.msea.2005.01.074]

Zhang, Y.H., van der Giessen, E., Nicola, L., 2010. Discrete dislocation simulations of the flattening of nanoimprinted surfaces. *Modelling and Simulation in Materials Science and Engineering*, **18**(3):034006. [doi:10.1088/0965-0393/18/3/034006]

Zong, Z., Lou, J., Adewoye, O.O., Elmustafa, A.A., Hammad, F., Soboyejo, W.O., 2006. Indentation size effect in the nano and microhardness of fcc single crystal metals. *Materials Science and Engineering: A*, **434**(1-2):178-187. [doi:10.1080/10426910601063410]